Journal of Materials Chemistry

Cite this: *J. Mater. Chem.*, 2012, **22**, 5715

www.rsc.org/materials

PAPER

SN@silicate: an anionic dye sorbent and its reuse†

Yan-Ping Wei and Hong-Wen Gao*

Received 24th November 2011, Accepted 13th January 2012
DOI: 10.1039/c2jm16132j

It is difficult for dye-synthesizing wastewater to be treated efficiently together with eco-friendly disposal of dye sludge. Octadecyl dimethyl hydroxyethyl quaternary ammonium (SN) was hybridized with magnesium silicate, and then characterized by various techniques. The SN bilayer stacking *via* hydrophobic interactions intercalated into the magnesium silicate sheets and caused an interlayer increase to 4.9 nm. More than 40% SN was embedded so that the hybrid contained a large number of positive charges and hydrophobic areas. It exhibited a faster adsorption to anionic dyes with higher capacities from 108 to 553 mg g^{-1} than for conventional sorbents. In addition, it captured microcystin-LR from water according to the lipid-water partition model. The resultant dye sludge was added into epoxy top coating and paint to fabricate colored films with an electric resistance decrease to 0.75×10^7 Ω. The facile preparation of such a functional material provided a "killing two birds with one stone" approach, from treatment of dye wastewater to disposal of the dye sludge, turning it to an antistatic colorant.

Introduction

In the past several decades, layered inorganic–organic hybrid materials have been studied extensively for not only fundamental interest and also many promising applications, such as ion exchange, catalysis, and construction of nanoscale assemblies, due to the ordered array of organic moieties within a stable inorganic matrix.[1] A challenge is to achieve particular properties by intercalating specific organic materials into a stable inorganic matrix. However, not all organic substances can be successfully intercalated into layered inorganic materials, which depends on their affinity. Recently, layered magnesium silicate host materials have received considerable interest because of their high resistance to acid, high surface area, high ion exchange, hydrophobic character, adsorption and molecular sieving properties.[2] Intercalation of organic guests in magnesium silicate leads to mesoporous materials and improves the adsorption capacity.[3–7] Surfactants are used extensively as guests in the shape-controlled synthesis of various functional materials, where they play the role of a soft template or stabilizer.[8–10] However, they ultimately have to be removed from the materials by washing with organic solvent or by calcination at high temperature.[11,12] As such this will cause waste during large-scale production.

In China, about 1.6 billion tons of dye-containing wastewater is produced every year, but only a small proportion is recycled.[13] Discharge of untreated dye wastewater leads to a serious threat to environmental safety including color pollution and toxicity to aquatic organisms.[14,15] Highly salt-like, recalcitrant dyes are resistant to degradation by microbiological processes, and it is difficult for dye wastewater to be treated effectively.[16] Flocculation and adsorption are often applied to pretreatment of dye wastewater; however, much dye sludge is produced and is usually disposed by landfill and incineration. Owing to the serious secondary pollution alone resulting from such conventional disposal, the reuse of dye sludge and synthesis of highly recyclable sorbents has attracted increased attention.[17] A possible solution is the use of inorganic–organic hybrids first to adsorb the organic pollutant and then to lead to useful materials. This may save resources and simultaneously reduce waste dye pollution, while the recovered material may remain unaffected in structure.

Octadecyl dimethyl hydroxyethyl ammonium, antistatic agent SN, was intercalated into magnesium silicate to form a hybrid material (Fig. 1A) and then utilised to adsorb dye-wastewater (Fig. 1B). The resultant sludge was added into paint and epoxy topcoating (EP) to form colored antistatic films (Fig. 1C) or calcined at 550 °C to form lamellar magnesium silicate sheets and reused as another sorbent.

Experimental section

Apparatus and materials

A photodiode array spectrometer (Model S4100, Scinco, Korea) with Labpro plus software (Firmware Version 060105) was used to determine the concentration of various dye solutions. A scanning electronic microscopy (SEM) (Model Quanta 200 FEG, FEI Co., USA) was used to measure the size and shape of

State Key Laboratory of Pollution Control and Resource Reuse, College of Environmental Science and Engineering, Tongji University, Shanghai, 200092, China. E-mail: EMSL@tongji.edu.cn; Fax: (+) 86-21-65988598
† Electronic supplementary information (ESI) available: Fig. S1–S11. See DOI: 10.1039/c2jm16132j

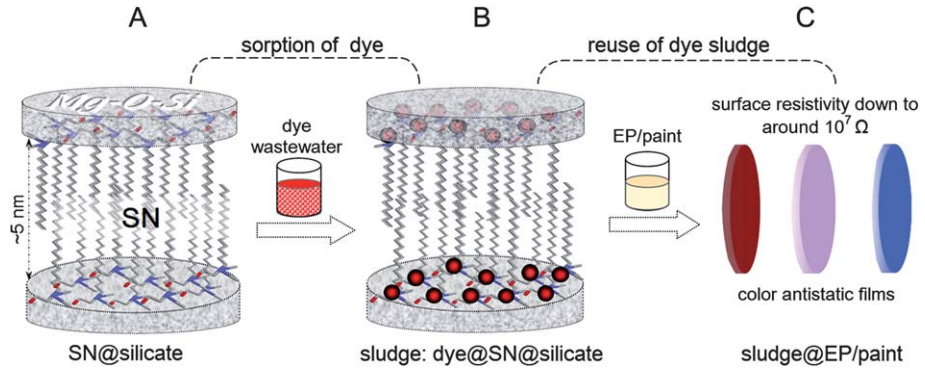

Fig. 1 Formation of the SN@silicate hybrid (A), sorption of dye (B) and reuse of dye sludge as antistatic agent added into EP/paint (C).

material particles. A transmission electron microscopy (TEM) with energy dispersive X-ray detector (Model TECNAI G2 S-TWIN, FEI Co., USA) was used to study surface morphology and element content of materials. The FT-IR spectra of the hybrids were obtained using an infrared spectrometer system (Model Equinoxss/hyperion 2000, BRUKER Co., Germany). Small-angle X-ray diffraction (SAXRD) (Model D/Max-2550 PC, Japan) spectra were recorded using Cu-Kα radiation in the range of ~1–10° 2θ at a voltage of 30 kV and current of 50 mA, and wide-angle X-ray diffraction (WAXRD) (Model Bruker D8 Advance, Germany) spectra were recorded in the range of ~10–90° 2θ at 40 kV and 40 mA. A thermal analysis system (Model Q600 SDT Simultaneous DSC/TGA, TA instruments, USA) was used for thermogravimetry analysis (TGA) of the materials. A ζ-potential instrument (Zetasizer Nano Z, Malvern, UK) was used to determine the surface potential of suspended materials. An inductively coupled plasma optical emission spectrometer (ICP-OES) (Model Optima 2100 DV, PerkinElmer, USA) was used to determine metal contents in materials. A total carbon analyzer (Model Elab-TOC, Elab, China) was used to determine total organic carbon (TOC) in dye wastewater. A high resistance meter (Model ZC36, Shanghai Precision Instruments Co., China) was used to determine the resistance of the EP/paint films.

Sodium metasilicate and magnesium nitrate (Aladdin Agents, China), SN (Zhejiang Runtu Co., Ltd, China) and microcystin-LR (MC-LR, 95–99%, Shanghai GreenEmpire EP S&T Co., China) were used for preparation of SNMSH samples. The adsorptions of thirteen kinds of ionic dyestuffs (Shanghai GreenEmpire EP S&T Co., China) on the SNMSH were investigated, which were classified into acidic/reactive, cationic/basic and amphoteric types. The acidic and reactive dyes included weak acid pink red B (APRB, C.I. 18073), weak acidic green GS (WAGGS, C.I. 61580), mordant red 3 (MR3, C.I. 58005), mordant blue 9 (MB9, C.I. 14855), acid green 25 (AG25, C.I. 61570), reactive brilliant red X-3B (X3B, C.I. 18200), direct blending scarlet DGLN (DGLN) and sirius red F3B (F3B, C.I. 60756). The cationic and basic dyes included basic brilliant blue BO (BBBO, C.I. 42595), ethyl violet (EV, C.I. 42600) and rhodamine B (RB, C.I. 45170) and the amphoteric ones, patent blue A (PBA, C.I. 42080) and patent blue VF (PBVF, C.I. 42045). The EP consisting of both liquid A and B units (Shanghai Lvjia Waterborne Coatings Co., China) and acrylic-based emulsion paint (Shanghai Akzo Nobel Swire Paints, China) were used to prepare the antistatic polymer films by mixing with the dye sludge.

Synthesis and characterization of SNMSH

The functionalized magnesium silicate material was synthesized following a precipitation method.[10] SN (0.178 M) was added into magnesium nitrate (0.2 M) under stirring, and then sodium silicate (0.2 M) added into the mixture quickly and mixed thoroughly. After settling, the suspension was centrifuged and washed with deionized water. Part of the product was dried and ground into powder, and the other part was diluted to a certain concentration after stirring. The addition mole ratio of SN : Mg : Si was 2 : 5 : 7. As reference, magnesium silicate was prepared according to the same procedure. The hybrid powder/liquid products were characterized by FTIR, XRD, TGA, SEM, TEM and ζ-potential analysis. Simultaneously, SEM of the SNMSH powder was measured after calcination at 550 °C. The SN content in the SNMSH was calculated by determining C content with an elemental analysis device; 0.2 mL of the SNMSH liquid was digested with a Fenton reagent (Aladdin Agents, China) and diluted to 25 mL. The concentrations of Mg and Si in the supernatant were determined by ICP-OES and the Mg and Si contents in the SNMSH were thus calculated.

Adsorption of dyes

0.1% (w/v) magnesium silicate or SNMSH were added into solutions containing cationic dyes *e.g.* EV and BBBO or anionic dyes *e.g.* APRB and WAGGS to study if selective adsorption was observed.

The adsorption capacities of the SNMSH to thirteen kinds of dyes were determined: 0.01% of SNMSH was added into anionic dye solutions *e.g.* PBA, MB9 and WAGGS from 10 to 120 μM, PBVF from 5 to 120 μM, MR3 from 20 to 240 μM, AG25 from 10 to 300 μM, X3B from 10 to 140 μM, APRB from 20 to 140 μM, and DGLN and F3B from 5 to 80 μM; similarly 0.1% of SNMSH was added into cationic dye solutions *e.g.* BBBO from 50 to 650 μM and RB from 5 to 500 μM. The SNMSH–dye mixtures were treated for 10 min with ultrasound. After the mixtures were centrifuged the concentrations of dyes in the supernatants were determined by spectrophotometry.

In addition, the influence of pH, ionic strength, temperature and time on the adsorption of WAGGS treated with SNMSH

were investigated. The temperature experiments from 10 to 50 °C were carried out in a constant temperature water-bath for 15 min. NaCl (1 M) was used to adjust ionic strength of the liquids from 0 to 0.2 M. The sorption time was carried out from 0 to 120 min. In all the experiments, the dye concentration in the supernatants were determined by spectrophotometry.

Adsorption of MC-LR

0.05% (w/v) of SNMSH was added into various solutions containing MC-LR from 0 to 2.8 mg L^{-1}. The solutions were mixed under ultrasound for 10 min. After centrifugation, the MC-LR concentration in the supernatants was determined with the microcystins plate kit (Shanghai GreenEmpire S&T Co., China).

Treatment of dye wastewater

Two kinds of unknown direct-blending dye (with more than two sulfonic groups) wastewaters (W1# and W2#) were sampled from Wujiang Tongluo Dyes Chem. Co. China. They were adsorbed by adding SNMSH from 0 to 1%. After separating the SNMSH-W1# sludge, the TOC and color of the supernatants were determined by a total organic carbon analyzer and spectrophotometry at 492 nm for W1# and 500 nm for W2#.

Reuse of dye sludge

The SNMSH-AG25 and SNMSH-APRB wet sludge was directly mixed with acrylic-based emulsion paint (EP) and then spread evenly on a plastic plate to a thickness of 250 μm with a spreader. Simultaneously, a reference paint-only film was prepared according the same method. After being room-dried, the surface electrical resistance of the films was determined with a high resistance meter. In addition, the W1# -SNMSH sludge was dried and powdered into particles of more than 200 mesh. 50 g of EP A liquid was mixed with 4 g of the sludge powder, and then 20 g of EP B liquid was added under stirring. The mixture was painted on a plastic plate and then the film room-dried. Simultaneously, a reference EP-only film was prepared. After the film surface was washed with alcohol, the surface electrical resistance of the EP films was determined. In order to observe the leaching of dye from the films, the W1# -SNMSH sludge - EP films were immersed into 2% HCl, 2% NaOH, tap water and ethanol for 70 days.

Results and discussion

Interaction of SN with magnesium silicate

Antistatic additive SN (octadecyl quaternary ammonium) is often added to synthetic fibers and plastics to improve the conductivity.[18] It is also an excellent cationic surfactant used in chemical industry. Magnesium silicate, known as talcum, is insoluble in dilute acidic or basic media, and is usually used as a lubricant added in plastic and cosmetics. From the interaction of SN with *in-situ* formed magnesium silicate, the embedded amount of SN increased with increase of SiO_3^{2-} and then approached an equilibrium state (see Fig. S1 A, ESI†). The adsorption obeyed the Langmuir isotherm model (see Fig. S1 B, ESI†), $c_e/q_e = 1/K_l q_\infty + c_e/q_\infty$,[6] where c_e *is* the equilibrium molarity of SN in mol L^{-1}, q_e adsorption amount of SN binding to magnesium silicate in mg g^{-1}, q_∞ the saturation amount of SN in mg g^{-1} and K_l the adsorption constant. This indicated monolayer binding of SN on the magnesium silicate, $(Mg_3Si_4O_{10})^{2-}$.[1] The q_∞ of SN was calculated as 1.1 g per g magnesium silicate, *i.e.* the content maximum of embedded SN in the SNMSH approached 52%; K was calculated to be 612 M^{-1}. Thus, the Gibbs free energy (ΔG) is <0, indicative of spontaneous interaction of the SN-magnesium silicate.

According to the recommended procedure, *i.e.* the initial mole ratio 1 : 0.4 : 1.5 of Mg^{2+} to SN and SiO_3^{2-} (see Fig. S1, ESI†), the SNMSH was formed and used. The molar ratio of Mg to SN and Si was calculated as 1 : 0.34 : 1.3 determined by element analysis and ICP-OES, and confirmed the formation of $SN@Mg_3Si_4O_{10}$, with approximately 45% SN embedding in the hybrid.

Characterization of the SNMSH

The FT-IR of the SNMSH supported the embedding of SN (Fig. 2). Comparison of curve 2 with 3 shows the IR characteristic bands of SNMSH appearing around 2917 cm^{-1} for $–CH_3$ and $–CH_2$ bands, 2849 cm^{-1} for symmetric stretching vibration of $–CH_2$, and 1470 cm^{-1} for asymmetric stretching vibration of $–CH_3$. From curve 2, the Mg–OH and Mg–O bands located at 3677 and 651 cm^{-1} indicated substantial OH− adsorbed on magnesium silicate with this weakened obviously in SNMSH. The C–N stretching vibration peak around 1100 cm^{-1} disappeared in the SNMSH indicating that the $>N^+$ of SN interacted with the negatively charged magnesium silicate sheets *via* electrostatic attraction. The Si–O band peak around 1018 cm^{-1} for magnesium silicate shifted to 1029 cm^{-1} for SNMSH which indicates that the Si–O bond participated in the interaction of SN with magnesium silicate.

From the change of the FTIR spectrum of SNMSH with pH (see Fig. S2, ESI†), it was observed that free-silica vibration bands at 1090 and 960 cm^{-1} and Si–OH band at 800 cm^{-1} appeared with decrease in pH while the Mg–OH band at 633 cm^{-1} disappeared at pH < 8;[5,6] Mg–OH was formed at pH > 9 so that SN bound to Mg–OH *via* electric attraction. The reaction liquid was adjusted to pH > 10 after the addition of

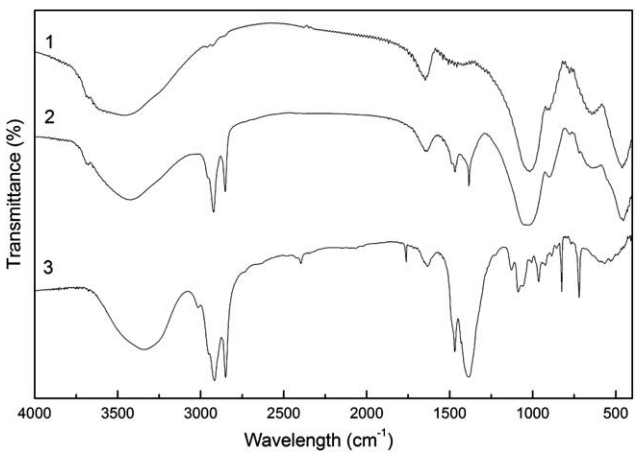

Fig. 2 FTIR spectra of magnesium silicate (1), SNMSH (2) and SN (3).

SiO_3^{2-} so that sufficient SN was embedded. From TGA curves (see Fig. S3 A, ESI†), the weight loss of the SNMSH is 42.5% between 190 and 532 °C, comparing with that of SN of >90% which is attributed to the decomposition of SN. The mass fraction of SN in the SNMSH was calculated to be 47%, which approached the above determination. From the differential thermogravimetry analysis (DTG) (see Fig. S3 B, ESI†), a broad peak appeared around 284 °C for SNMSH and confirmed the intermolecular interaction between SN and the magnesium silicate sheets. Magnesium silicate has a lamellar structure (ϕ = 80–150 nm) (Fig. 3A). With addition of SN, rope-like particles with 5–15 μm size (see Fig. S4, ESI†) were formed and aggregated together vertically (Fig. 3B and C). From SEM images of the SNMSH calcined to decompose completely the SN at 550 °C, lamellar magnesium silicate (ϕ 50–100 nm, thickness <5 nm) was formed during the hybridization of SN (see Fig. S5 A, ESI†). The presence of SN clearly affected the stacking of lamellar magnesium silicate; TEM reveals that SN (white spots) was distributed evenly in the porous magnesium silicate net (Fig. 3D). Parallel line-like, lamellar SN (confirmed with EDX) was observed in the interior of the hybrid (Fig. 3E). The ζ-potential of magnesium silicate alone was determined to be −45.5 mV in aqueous media and can be attributed to significant absorption of OH^- in basic media *via* the interaction with Mg^{2+} and O–Si.[1] After the intercalation of SN, the ζ-potential of the SNMSH changed to +29.6 mV. Therefore, electrostatic interaction occurred between SN^+ and OH^- of the lamellar magnesium silicate (Fig. 3F).[19] When the polar head of SN approached the magnesium silicate sheets, a hydrogen bond *e.g.* O–H···O–Si will be formed between $-C_2H_4OH$ of SN and O–Si of the lamellar sheets. Further, the space between adjacent magnesium silicate sheets was 4.98 nm (Fig. 3E), well consistent with SAXRD-based calculation below. This distance corresponds to double the SN molecular length. Thus, a SN bilayer may form between the magnesium silicate sheets *via* hydrophobic interaction of the long alkyl chains (Fig. 3F), similar to the phospholipid bilayer of cell membranes.[20] Thus, the SN bilayer intercalated between the magnesium silicate sheets *via* these non-covalent interactions to form the SNMSH positively charged layer.[21,22]

The XRD of SNMSH is similar to reported magnesium organosilicate materials (Fig. 4B).[1,3,23,24] The intralayer reflection (d_{060} 1.56 Å) is characteristic of the 2 : 1 trioctahedral phyllosilicate structure. Both magnesium silicate and its SN hybrid show the same intralayer reflection (d_{060}). This indicates that SN is accommodated in the layered inorganic framework without the loss of long-range periodicity.[1] Curve 2 exhibits the same peak location as curve 1. The main structure of the hybrid remains unchanged after the hybridization of SN. The d_{001} values of magnesium silicate and its SN hybrid are 1.435 and 4.906 nm (Fig. 4A), where the former is similar to the layered talc $[Mg_3Si_4O_{10}(OH)_2]$ structure.[23] After the hybridization of SN, d_{001} is much enlarged, approximately double the alkyl chain length (about 25 Å) of SN. Therefore, the SN bilayer was formed by intercalation between the magnesium silicate sheets.[25]

Adsorption of dyes on the SNMSH

From the above analysis, the SNMSH carries a great deal of positive charges. It may thus be expected to adsorb strongly anionic organic compounds, *e.g.* acidic or reactive dyes. With addition of the SNMSH into APRB, WAGGS, EV and BBBO solutions, the SNMSH adsorbed all these dyes based on the color change of the supernatants while magnesium silicate showed adsorption selectivity to only BBBO and EV (see Fig. S6, ESI†). From curve 3 in Fig. 4, the adsorption of dye *e.g.* WAGGS hardly changed the thickness of the SN intralayer. The sorption of anionic dye is attributed to the electrostatic interaction with SN embedded in the hybrid, which was confirmed by the ζ-potential change from +29.6 to −8.94 mV. According to the recommended method, the adsorptions of thirteen dyestuffs were

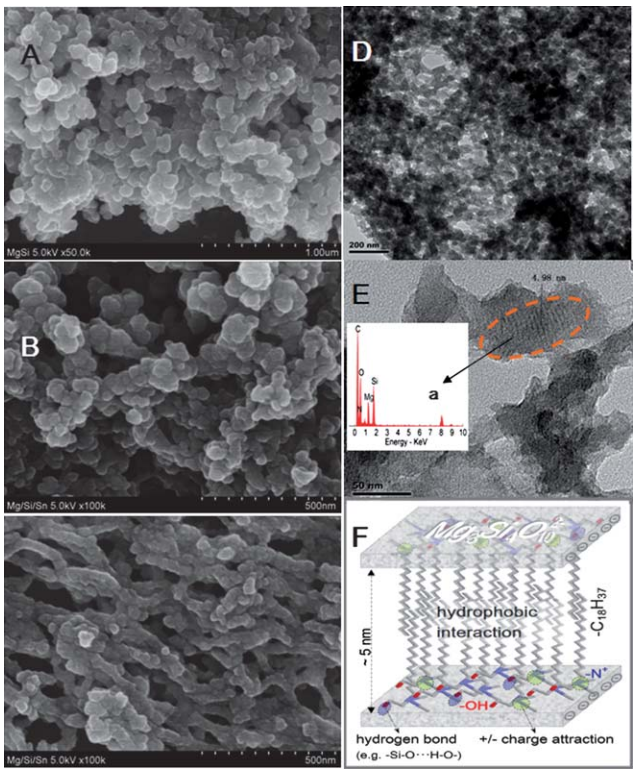

Fig. 3 SEM of magnesium silicate alone (A) and of SNMSH (B, C). TEM of the SNMSH material (D, E). E-a: EDX of the layered area, F: cartoon illustration of SNMSH with the intermolecular interaction.

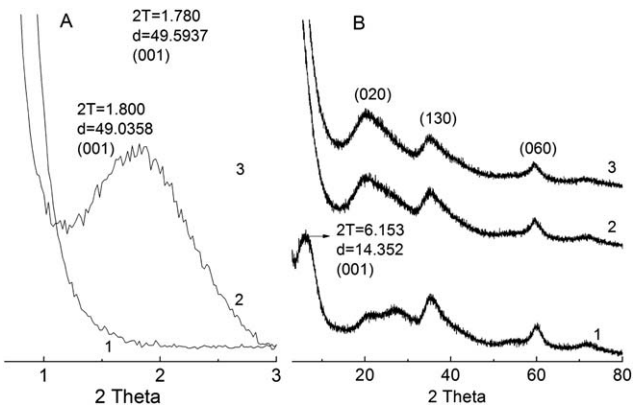

Fig. 4 SAXRD (A) and WAXRD (B) of magnesium silicate (1), the SNMSH material (2) and the WAGGS-SNMSH sludge (3).

determined and the experimental data fitted to the Langmuir isotherm model except for MB (see Fig. S7, ESI†). The q_∞ of each dye binding to the SNMSH was calculated as given in Table 1, where the charge number (n) and the octanol/water partition coefficient ($K_{o/w}$) are also included.

From q_∞ values in Table 1, the SNMSH has a higher absorption capacity to anionic dyes, *e.g.* acidic, reactive and amphoteric dyes. For example, q_∞ values of WAGGS, X3B, APRB and PBA are over 300 mg g^{-1}. The adsorption amounts of anionic dyes on the SNMSH are much higher than those of the other sorbents reported (Table 1). Different from active carbon, the positive-negative charge interaction plays a dominant role in these adsorptions. Among these sulfonic dyes, q_∞ values are not relevant to the charge number *e.g.* 253 mg g^{-1} for DGLN and 261 mg g^{-1} for F3B, and also the positively charged amino group hardly affected the adsorption, *e.g.* two amphoteric dyes. From Table 1, q_∞ values were positively related to the lg $K_{o/w}$ value *e.g.* 368 mg g^{-1} for WAGGS (lg $K_{o/w}$ = 5.88), 400 mg g^{-1} for APRB (lg $K_{o/w}$ = 4.72), compared to only 121 mg g^{-1} for MB9 (lg $K_{o/w}$ = 0.026). Hydrophobic interaction occurred between the hydrophobic groups of dye and the long alkyl chains of embedded SN in the SNMSH besides the electric charge interaction. Therefore, the sulfonic dyes with more hydrophobic groups are more easily adsorbed in the SNMSH. Besides anionic dyes, the basic/cationic dyes were adsorbed on the SNMSH but their capacities were much less than those of anionic dyes. The capacity is positively related to the $K_{o/w}$ value, *e.g.* 103 mg g^{-1} for BBBO (lg $K_{o/w}$ = 4.21) and only 12 mg g^{-1} for MB (lg $K_{o/w}$ = −1.13). Therefore, they may interact with only the long alkyl chains of SN owing to the repulsion of like electric charges. From the relationship among $K_{o/w}$, n and q_∞ (see Fig. S8, ESI†), such anionic dyes with a high hydrophobicity *e.g.* $K_{o/w}$ >10 L kg^{-1} often exhibit the higher adsorption capacity. On the contrary, cationic dyes always show a low capacity even if with a high hydrophobicity.

The ζ-potential of the SNMSH increased with decrease of pH from 12 to 8, *e.g.* +24 mV at pH 10 up to +40 mV at pH 8, and then approached almost constant value at pH < 8 (see Fig. S9, ESI†). So it is more favorable for anionic dye to be adsorbed in low pH solution. WAGGS as a representative anionic dye was selected to investigate the effect of the reaction conditions. The adsorption of WAGGS decreased slightly with increase of pH from 1 to 3 and then approached an almost constant value (see Fig. S10 A, ESI†). The effect of ionic strength indicated that a highly salt media is favorable for the adsorption of WAGGS (see Fig. S10 B, ESI†). This is attributed to the fact that ionic strength can strengthen the hydrophobic interaction between WAGGS and SN. Temperature little affected the adsorption of WAGGS (see Fig. S10 C, ESI†). Thus, the SNMSH may adsorb effectively anionic dye in any season from highly salt solution and for any acidity or alkalinity wastewater. The adsorption rate of WAGGS was >60% in the first 5 min and >80% in 1 h (see Fig. S10 D, ESI†); the positive–negative charge attraction accelerated the adsorption of anionic dyes.

Adsorption of MC with SNMSH

Besides the ionic dyes above, hydrophobic organic contaminants *e.g.* persistent organic pollutants (POPs) may be adsorbed owning to a great deal of SN embedded in the SNMSH. As an example of hydrophobic environmental contaminants, MCs are cyclic non-ribosomal peptides produced by several species of cyanobacteria,[38] where MC-LR is the most abundant and most toxic worldwide. It inhibits protein phosphatase type 1 and 2A,[39] has demonstrated tumor-promoting activity[40] and causes developmental toxicity.[20] A few studies have suggested a relationship between liver and colorectal cancers and the occurrence of cyanobacteria in drinking water.[41] MC-LR contains many hydropbobic alkyl side-chains and three polar side-chains *e.g.* two carboxyl groups and two amino groups (Fig. 5A). Owing to its

Table 1 The adsorption capacity of the SNMSH to ionic dyes with $K_{o/w}$ and comparison with the other sorbents reported

			q_∞			q_∞ comparison	
Category	Dye	Charge number, n	mmol g^{-1}	mg g^{-1}	lg $K_{o/w}$[a]	Sorbent	q_∞/mg g^{-1}
Acidic/reactive dyes	MR3	1−	0.77	264	−2.47	Modified silica[26]	148
	MB9	2−	0.24	121	0.026		
	WAGGS	2−	0.52	368	5.88	Trametes versicolor[27]	104
	AG25	2−	0.47	293	3.05	Activated carbon[28]	280
						Activated palm ash[29]	123
						Acid treated coconut husk[30]	46.6
	X3B	2−	0.56	345	1.27	Metal hydroxide sludge[31]	62.5
	APRB	2−	0.59	400	4.72	$CaCO_3$ hybrid[32]	221
						Rice bran[33]	0.85
	DGLN	5−	0.20	253	3.33		
	F3B	6−	0.19	261	3.3	Soy meal hull[34]	179
						Mixture almond shells[35]	22.4
Amphoteric dyes	PBA	2−/1+	0.80	553	−0.23	Activated clay/carbons mixture[36]	64.7
	PBVF	2−/1+	0.19	108	−2.47		
Cationic/basic dyes	MB	1+	0.036	12	−1.13		
	BBBO	1+	0.20	103	4.21		
	RB	1+	0.15	72	2.74		

[a] The octanol/water partition coefficient, calculated with the Molinspiration Cheminformatics[37]

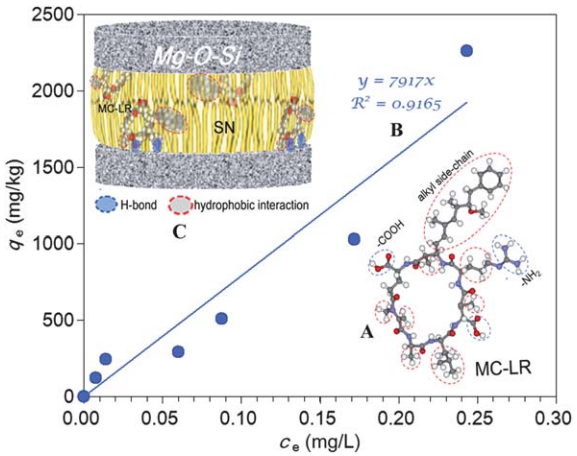

Fig. 5 Chemical structure of MC-LR (A), its adsorption curve on SNMSH (B) and illustration of its interaction with SNMSH (C).

stable chemical property *i.e.* lg $K_{o/w} = 3.67$,[42] it is difficult for MC-LR to be removed from drinking water by conventional methods, *e.g.* flocculation and disinfection.

The experimental results showed that the adsorption of MC-LR with SNMSH fitted the lipid-water partition model (Fig. 5B), *i.e.* $q_e = K_{h/w}c_e$ where $K_{h/w}$ is the partition coefficient of MC-LR in L kg^{-1}. The hydrophobic groups of MC-LR no doubt play a dominant role in such binding, *i.e.* the alkyl side-chains of MC-LR inserted within the long alkyl chains of SN *via* hydrophobic interaction (Fig. 5C); additionally hydrogen bonds may be formed simultaneously between $-NH_2$ or –COOH of MC-LR and Si–O of the magnesium silicate sheets (Fig. 5C). The $K_{h/w}$ of MC-LR was calculated to be 7917 L kg^{-1}, *i.e.* lg $K_{h/w} = 3.90$, which is more than lg $K_{o/w}$. Only 500 mg L^{-1} of the SNMSH can capture more than 80% of MC-LR contaminant and therefore is an efficient sorbent for MCs.

Treatment of dye waste

Two direct-blending dye wastewaters sampled from Wujiang Tongluo Dyes Chem. Co. were treated with SNMSH. The dyes with more than two sulfonic groups were readily adsorbed by the SNMSH. From the change of the column height in Fig. 6, the colority and TOC decreased obviously with increase of the SNMSH. For example, the removal rates of colority and TOC of W1# (*i.e.* highly concentrated dye wastewater) reached 92% and 72% with addition of 0.5% of the SNMSH (Fig. 6A). In addition, only 0.1% of the SNMSH added has removed 88% of colority and 68% of TOC from W2# (*i.e.* low concentration dye wastewater) (Fig. 6B). This demonstrates that the SNMSH is an efficient sorbent for treatment of dye wastewater.

Over the years, it has been difficult to be dispose of solid organic waste in an eco-friendly way. During treatment of dye wastewater, plenty of color sludge is often produced. The conventional disposal *e.g.* landfill and incineration often cause the secondary pollution of air and ground water. Reuse of organic sludge is becoming a hot topic in water pollution control.[43] As is well known, electrostatic charges of *e.g.* plastic and fiber products are a nuisance and may even cause fire or explosions in factories and mines. Antistatic agents are often used in plastic and textiles but most of them are sticky fluids when a solid material dispersion is more favorable. In the above dye sludge, the content of SN is more than 30%. If it was added in polymer *e.g.* EP or acrylic-based paint, the antistatic performance of polymer might be improved. According to the recommended procedure, the W1#, AG25 and APRB sludges formed with the SNMSH were added in EP and acrylic-based emulsion paint. The dye sludge paints were spread on plastic plates to form smooth and even colored films (Fig. 7). The surface electrical resistance of the EP films was determined to be 0.51 × 10^{10} Ω without any additive and 0.18 × 10^{8} Ω with the W1# sludge (Fig. 7). The resistivity of the dye sludge – EP film was the lowest, approximately three-hundredth of the EP-only film value. The resistivities of the paint films were 0.70 × 10^{8} Ω without any additive, 0.20 × 10^{8} Ω with the AG25 sludge and 0.75 × 10^{7} Ω with the APRB sludge (Fig. 7).

The EP-W1#-SNMSH film was immersed into tap water, ethanol, 2% NaOH and 2% HCl for 70 days. A faint color appeared in the acidic and basic media but no color was leached from the films in the other solutions (see Fig. S11, ESI†). It indicated that organic substance *e.g.* dye was immobilized firmly in the EP film. Thus, it is feasible for the dye sludge to be reused as an antistatic polymer additive. This may decrease seriously the

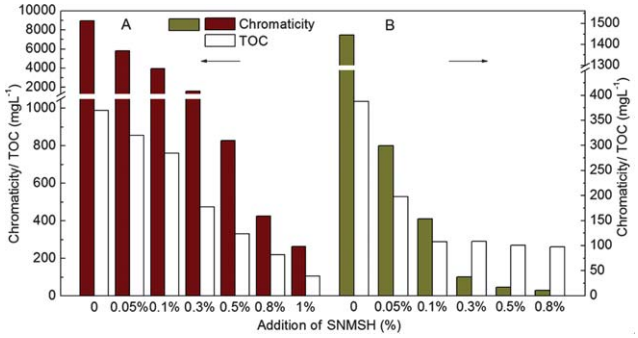

Fig. 6 Treatment of direct-blending dye-manufacturing wastewaters: W1# (A) and W2# (B) with SNMSH.

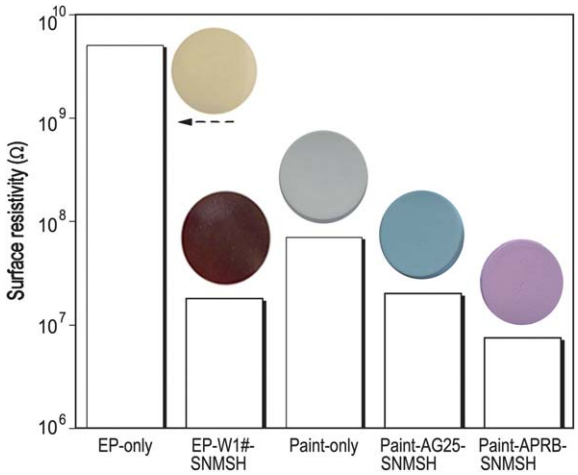

Fig. 7 Surface resistivity of EP-only, EP-W1#-SNMSH sludge, paint-only, paint-AG25-SNMSH sludge and paint-APRB-SNMSH sludge films together with photos.

formation of highly toxic intermediate products and release of large amounts of carbon oxide resulting from an advanced photocatalysis or oxidation processes[14] so reducing waste of resources.

In addition, the dye-SNMSH sludge was calcined at 550 °C and a lamellar silicate (ϕ = 50–100 nm) formed with flat surface and ultrathin thickness (<5 nm) (see Fig. S5 B, ESI†). It retains the same morphology as magnesium silicate (Fig. 3A). Therefore, the inorganic–organic hybrid may be used to adsorb organic pollutants before calcination and the morphology of the final material remains unaffected. The calcined material may be used as a sorbent for dyes and fluoride.[44,45] Besides, it should be a good non-halogenated flame-retardant, which may be added in plastic electric wire and cable.

Conclusions

In previous work, a number of inorganic–organic hybrids with plenty of negative charges were synthesized though they adsorbed only cationic dyes.[43,46] By the hybridization of SN into magnesium silicate, a hybrid material with plenty of positive charges has been prepared in the present work, where the SN bilayer intercalated into the magnesium silicate sheets *via* charge attraction, hydrogen bonding and hydrophobic interaction. Such a material appeared simultaneously multifunctional showing, *e.g.* adsorption, complexation, ionic exchange and flocculation. From the adsorptions of thirteen ionic dyes, the SNMSH exhibited a high adsorption capacity towards anionic and amphoteric dyes, where the electrostatic interaction plays a dominant role. In addition, it adsorbed MCs *via* the hydrophobic interaction according to the lipid–water partition model with a high $K_{h/w}$ of 7917 L kg^{-1}. The dye –SNMSH sludge can be reused as an antistatic agent added in EP and paint, and the surface electrical resistance of films decreased down to 0.75 × 10^7 Ω. This work has provided a novel recycling approach of a sustainable functionalized material for treatment of dye wastewater together with eco-friendly disposal of dye sludge.

Abbreviations

APRB	weak acid pink red B
WAGGS	weak acidic green GS
MR3	mordant red 3
MB9	mordant blue 9
AG25	acid green 25
X3B	reactive brilliant red X-3B
DGLN	direct blending scarlet DGLN
F3B	sirius red F3B
BBBO	basic brilliant blue BO
EV	ethyl violet
RB	rhodamine B
PBA	patent blue A
PBVF	patent blue VF
EP	epoxy topcoating
SN	octadecyl dimethyl hydroxyethyl quaternary ammonium
SNMSH	SN-magnesium silicate hybrid
TOC	total organic carbon
SAXRD	small-angle X-ray diffraction
WAXRD	wide-angle X-ray diffraction
ICP-OES	inductively coupled plasma optical emission spectrometer
SEM	scanning electronic microscopy
TEM	transmission electron microscopy
MC-LR	microcystin-LR

Acknowledgements

We thank the Foundation of State Key Laboratory of Pollution Control and Resource Reuse (Tongji University), China (No. PCRRK11003) for financially supporting this work.

Notes and references

1 S. L. Burkett, A. Press and S. Mann, *Chem. Mater.*, 1997, **9**, 1071–1073.
2 F. Ciesielczyk, A. Krysztafkiewicz and T. Jesionowski, *J. Mater. Sci.*, 2007, **42**, 3831–3840.
3 R. K. Dey, A. S. Oliveira, T. Patnaik, V. K. Singh, D. Tiwary and C. Airold, *J. Solid State Chem.*, 2009, **182**, 2010–2017.
4 F. Ciesilelczyk, A. Krysztafkiewicz and T. Jesionowski, *Physicochem. Probl. Miner. Process.*, 2007, **41**, 185–193.
5 C. F. Du and H. M. Yang, *Clays Clay Miner.*, 2009, **57**, 290–301.
6 S. K. Parida, S. Dash, S. Patel and B. K. Mishra, *Adv. Colloid Interface Sci.*, 2006, **121**, 77–110.
7 A. Mierczynska-Vasilev and D. A. Beattie, *J. Colloid Interface Sci.*, 2010, **344**, 429–437.
8 S. R. Gajjela, K. Ananthanarayanan, C. Yap, M. Gratzel and P. Balaya, *Energy Environ. Sci.*, 2010, **3**, 838–845.
9 Y. Zhou, M. Kogiso and T. Shimizu, *J. Am. Chem. Soc.*, 2009, **131**, 2456–2457.
10 Q. Zhang, W. T. Yao, X. Y. Chen, L. W. Zhu, Y. B. Fu, G. B. Zhang, L. Sheng and S. H. Yu, *Cryst. Growth Des.*, 2007, **7**, 1423–1431.
11 S. J. Wu, F. T. Li, Y. N. Wu, R. Xu and G. T. Li, *Chem. Commun.*, 2010, **46**, 1694–1696.
12 J. Y. Xiao and L. M. Qi, *Nanoscale*, 2011, **3**, 1383–1396.
13 L. Brindley, *Chem. World*, 2009-07-08.
14 V. K. Gupta and Suhas, *J. Environ. Manage.*, 2009, **90**, 2313–2342.
15 J. S. Bae and H. S. Freeman, *Dyes Pigm.*, 2007, **73**, 81–85.
16 G. Crini, *Bioresour. Technol.*, 2006, **97**, 1061–1085.
17 Z. Song, L. F. Chen, J. C. Hu and R. Richards, *Nanotechnology*, 2009, 20.
18 L.-x. Huang, Q.-f. An and L.-s. Li, *China Surfactant Detergent & Cosmetics*, 2004, **34**, 308–311.
19 A. Monnier, F. Schuth, Q. Huo, D. Kumar, D. Margolese, R. S. Maxwell, G. D. Stucky, M. Krishnamurty, P. Petroff, A. Firouzi, M. Janicke and B. F. Chmelka, *Science*, 1993, **261**, 1299–1303.
20 C. Song, H. W. Gao and L. L. Wu, *Toxicol. Sci.*, 2011, **122**, 395–405.
21 A. W. Xu, M. Antonietti, H. Cölfen and Y. P. Fang, *Adv. Funct. Mater.*, 2006, **16**, 903–908.
22 D. Kuang, A. Xu, Y. Fang, H. Liu, C. Frommen and D. Fenske, *Adv. Mater.*, 2003, **15**, 1747–1750.
23 N. T. Whilton, S. L. Burkett and S. Mann, *J. Mater. Chem.*, 1998, **8**, 1927–1932.
24 R. Bharathwaj, U. Natarajan and R. Dhamodharan, *Appl. Clay Sci.*, 2010, **48**, 300–306.
25 R. Guegan, *Langmuir*, 2010, **26**, 19175–19180.
26 T. Jesionowski, A. Przybylska, B. Kurc and F. Ciesielczyk, *Dyes Pigm.*, 2011, **89**, 127–136.
27 Y. X. Wang and J. Yu, *Water Sci. Technol.*, 1998, **38**, 233–238.
28 E. Guibal, P. McCarrick and J. M. Tobin, *Sep. Sci. Technol.*, 2003, **38**, 3049–3073.
29 B. H. Hameed, A. A. Ahmad and N. Aziz, *Chem. Eng. J.*, 2007, **133**, 195–203.

30 H. N. A. Halim and N. S. M. Yatim, in *2011 International Conference on Environment and Industrial Innovation*, IACSIT Press, Singapore, 2011, pp. 268–272.
31 S. Netpradit, P. Thiravetyan and S. Towprayoon, *Water Res.*, 2003, **37**, 763–772.
32 D. H. Zhao, Y. L. Shen, Y. L. Zhang, D. Q. Wei, N. Y. Gao and H. W. Gao, *J. Mater. Chem.*, 2010, **20**, 3098–3106.
33 S. Hashemian, S. Dadfarnia, M. Nateghi and F. Gafoori, *Afr. J Biotechnol*, 2008, **7**, 600–605.
34 M. Arami, N. Y. Limaee, N. M. Mahmoodi and N. S. Tabrizi, *J. Hazard. Mater.*, 2006, **135**, 171–179.
35 F. D. Ardejani, K. Badii, N. Y. Limaee, S. Z. Shafaei and A. R. Mirhabibi, *J. Hazard. Mater.*, 2008, **151**, 730–737.
36 Y. S. Ho, C. C. Chiang and Y. C. Hsu, *Sep. Sci. Technol.*, 2001, **36**, 2473–2488.
37 L. Su, J. Yang, Y.-q. Wang and G.-j. Wang, *J. China Pharm. Univ.*, 2008, **39**, 178–182.
38 C. Djediat, M. Malecot, A. de Luze, C. Bernard, S. Puiseux-Dao and M. Edery, *Toxicon*, 2010, **55**, 531–535.
39 M. Tachi, S. Y. Imanishi and K. I. Harada, *Environ. Toxicol.*, 2007, **22**, 620–629.
40 N. Q. Gan, X. Y. Sun and L. R. Song, *Chem. Res. Toxicol.*, 2010, **23**, 1477–1484.
41 L. Zhou, H. Yu and K. Chen, *Biomed. Environ. Sci.*, 2002, **15**, 166–171.
42 M. M. Gehringer, P. Milne, F. Lucietto and T. G. Downing, *Environ. Toxicol. Pharmacol.*, 2005, **19**, 297–303.
43 Y.-P. Wei, D.-Q. Wei and H.-W. Gao, *Chem. Eng. J.*, 2011, **172**, 872–878.
44 A. Krysztafkiewicz, S. Binkowski and T. Jesionowski, *Appl. Surf. Sci.*, 2002, **199**, 31–39.
45 P. Y. Zhu, H. Z. Wang, B. W. Sun, P. C. Deng, S. Q. Hou and Y. W. Yu, *J. Chem. Technol. Biotechnol.*, 2009, **84**, 1449–1455.
46 J. Lin and H. W. Gao, *J. Mater. Chem.*, 2009, **19**, 3598–3601.

